Proceedings Paper:

Paspatis, A.G., Konstantopoulos, G.C. orcid.org/0000-0003-3339-6921, Mayfield, M. orcid.org/0000-0002-9174-1773 et al. (1 more author) (2018) Current-limiting droop controller with fault-ride-through capability for grid-tied inverters. In: 2017 IEEE PES ISGT Europe Conference Proceedings. 7th IEEE International Conference on Innovative Smart Grid Technologies (IEEE PES ISGT Europe 2017), 26-29 Sep 2017, Torino, Italy. IEEE . ISBN 978-1-5386-1954-4

https://doi.org/10.1109/ISGTEurope.2017.8260159

Current-Limiting Droop Controller with Fault-Ride-Through Capability for Grid-Tied Inverters

A. G. Paspatis, G. C. Konstantopoulos
Dept. Automatic Control and Systems Engineering
The University of Sheffield
Sheffield, UK
{apaspatis1, g.konstantopoulos}@sheffield.ac.uk

M. Mayfield
Dept. Civil and Structural Engineering
The University of Sheffield
Sheffield, UK
martin.mayfield@sheffield.ac.uk

V. C. Nikolaidis
Dept. Electrical and Computer Engineering
Democritus University of Thrace
Xanthi, Greece
vnikolai@ee.duth.gr

***Abstract*—In this paper, the recently proposed current-limiting droop (CLD) controller for grid-connected inverters is enhanced in order to comply with the Fault-Ride-Through (FRT) requirements set by the Grid Code under grid voltage sags. The proposed version of the CLD extends the operation of the original CLD by fully utilizing the power capacity of the inverter under grid faults. It is analytically proven that during a grid fault, the inverter current increases but never violates a given maximum value. Based on this property, an FRT algorithm is proposed and embedded into the proposed control design to support the voltage of the grid. In contrast to the existing FRT algorithms that change the desired values of both the real and reactive power, the proposed method maximizes only the reactive power to support the grid voltage and the real power automatically drops due to the inherent current-limiting property. Extensive simulations are presented to compare the proposed control approach with the original CLD under a faulty grid.**

***Index Terms*—Inverter, droop control, current-limiting property, fault-ride-through, voltage sags**

I. Introduction

DURING the last decades, the integration of distributed energy resources (DERs) into the power network has significantly increased. Despite the environmental, economical and social advantages offered by their usage, technical issues related to the stability of the grid have been raised. The vast majority of the DERs use power electronic devices for their connection with grid and therefore the control design of these devices is crucial for the stability of the power network. The most commonly used technique for inverters to support the grid is the droop control methodology, which adjusts the output real and reactive power of the inverter when the grid voltage and frequency change [19], [16].

Several droop control techniques have been proposed in the literature, where the droop functions have to be modified depending on the type of the output impedance of the inverter [10], [12]. Traditionally, inverters introduce an inductive output impedance and the real power is mainly related to the frequency of the grid, while the reactive power is related to the grid voltage. This introduces the well-known $P \sim \omega$ and $Q \sim V$ droop functions as stated in [6]. These droop functions are usually defined by the Grid Code [15] and should be satisfied by every grid-connected inverter under a normal grid operation. However, in low voltage networks or in the cases where a virtual resistance is introduced via the control design, the droop expressions are modified as $P \sim V$ and $Q \sim -\omega$ [25], [8], [11]. Such a droop control method has been recently introduced in [24] as the current-limiting droop controller (CLD) and can additionally guarantee a limited current during grid faults. The necessity for current-limiting control and the instability phenomena that may arise from conventional current-limiting techniques, especially under grid faults, have been underlined in [17], [2].

Furthermore, when faults occur in the grid, most of the DERs will continue injecting active power to the grid, usually with a high current, which negatively affects the protection system operation and can cause damage to the grid infrastructure [1]. The large currents result in a harmful stressing not only of the grid but of the interface device (inverter) as well. However, the current practice for protecting the DERs can cause them to desynchronize, disconnect or stop acting as a source during short circuit or a voltage sag. In most of the cases, faults are being cleared by the system in a very short time period and the desynchronization or disconnection of the DERs decreases the efficiency of the system. Therefore, for the conventional synchronous generators, fault-ride-through (FRT) techniques have been applied based on the use of conventional automatic voltage regulators (AVRs) [15]. In the same framework, DERs are required to follow similar FRT requirements under faulty grid conditions. In 2008, BDEW published guidelines for the connection of DERs at the medium voltage network providing details on the function of each DER when the point of common coupling (PCC) experiences a voltage drop [3]. These guidelines were supplemented in 2011 and 2013, and were then adopted by ENTSO-E, thus expanding them to the entire European supergrid [9]. In 2009, National Grid introduced similar guidelines for the UK transmission network (Grid Code) [14].

Extended research in complying the DER controller with FRT requirements can be found in the literature. In [13], BDEW guidelines are considered to support the voltage during a grid fault. When non symmetrical faults occur, conventional reactive support is not enough since positive or negative sequence reactive power strategies should be followed in order for the faulty phase/phases to return to their rated values, as stated in [7], [5]. The sequence-depended strategies are being extensively used due to the flexibility that they provide to the system. In [21], the importance of the FRT gain is being stated and different techniques for setting the maximum injected active current during fault are shown, while in [4], different power references are being set according to the desired ride-though strategy. Recently, increasing interest is shown in incorporating the FRT requirements into single-phase systems, such as in [23], [22], where the orthogonal signal generator (OSG)-based PLL principle is used to control a single-phase PV system under grid faults. As a result, there exist different FRT control schemes to support the power grid via reactive power injection; however, to the best of our knowledge, in order for these methods to be implemented in combination with a droop control strategy, a switching action between the two separate control dynamics is required, which can lead to integration windup and instability [17], [2].

In this paper, an enhanced version of the CLD controller is proposed for grid tied inverters to satisfy the FRT requirements under voltage sags of the PCC in a unified structure. Opposed to the original CLD which limits the current under a lower value when a voltage sag occurs, the proposed controller fully utilizes the capacity of the inverter, maximizing the injected current during a fault. The current-limiting property is analytically shown based on nonlinear systems theory. This allows the implementation of the FRT technique inside the controller dynamics in order to fully support the grid under significant voltage drops. It is proven that only the reactive power reference is adjusted during a grid fault, while the real power automatically reduces to its minimum value due to the inherent current-limiting property of the proposed CLD. It is also shown that the proposed controller can change the operation of the inverter between three modes: i) droop control, ii) accurate real and reactive power regulation to their reference values and iii) FRT, with a guaranteed current-limiting property at all times. Extensive simulations are presented to verify the efficiency of the proposed controller.

The paper is organized as follows: In Section II, the problem is stated and the background of the CLD and the FRT requirements is presented. In Section III, the proposed controller is introduced and the current-limiting property is mathematically proven. In Section IV, simulation results are presented to illustrate the functionality of the proposed controller while conclusions are given in Section V.

II. Problem Formulation

A. Review of Current-Limiting Droop Control

In Fig. 1, the system under investigation is shown. It consists of an inverter with an LCL filter connected to the grid. The filter inductances are denoted as L and L_g in series with the small parasitic resistances r and r_g, respectively, while the filter capacitance is C with a large parasitic resistance R_c in parallel. The output voltage and current of the inverter are v and i, respectively.

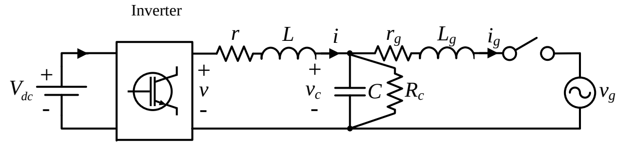

Figure 1. The inverter connected to the grid via an LCL filter

The dynamic equations of the system can be obtained as

$$\begin{aligned} L\frac{di}{dt} &= -ri + v - v_c \\ C\frac{dv_c}{dt} &= i - \frac{v_c}{R_C} - i_g \\ L_g\frac{di_g}{dt} &= v_c - r_g i_g - v_g, \end{aligned} \tag{1}$$

where the control input is represented by the inverter voltage v. According to [24], the CLD is defined using the droop functions for inverters with a resistive output impedance [25] as follows:

$$v = v_c + (1 - w_q)(\sqrt{2}V_g \sin(\omega_g t + \delta) - wi), \tag{2}$$

where V_g and ω_g are obtained from a traditional phase-locked-loop (PLL), while w, w_q, δ and δ_q dynamically change according to the expressions

$$\dot{w} = -c_w(K_e(E^* - V_c) - n(P - P_{set}))w_q^2 \tag{3}$$

$$\dot{w}_q = \frac{c_w(w - w_m)w_q}{\Delta w_m^2}(K_e(E^* - V_c) - n(P - P_{set})) - k_w\left(\frac{(w - w_m)^2}{\Delta w_m^2} + w_q^2 - 1\right)w_q \tag{4}$$

$$\dot{\delta} = c_\delta(\omega^* - \omega_g + m(Q - Q_{set}))\delta_q^2 \tag{5}$$

$$\dot{\delta}_q = -\frac{c_\delta \delta \delta_q}{\Delta \delta_m^2}(\omega^* - \omega_g + m(Q - Q_{set})) - k_\delta\left(\frac{\delta^2}{\Delta \delta_m^2} + \delta_q^2 - 1\right)\delta_q. \tag{6}$$

It is proven in [24] that the CLD limits the RMS value of the inverter current under a given value without any limiters or external devices that could cause instability [18]. For further information about (3)-(6), see [24].

However, the maximum capacity of the inverter is not utilized when the grid voltage drops, e.g. under grid faults, and the current is limited below a lower value that corresponds to the same voltage drop as the grid voltage. Hence, in cases of faults in the grid, the reactive power cannot be maximized to provide support to the grid, as imposed by the FRT requirements.

B. Fault-Ride-Through Requirements

The Fault-Ride-Through Requirements have been proposed for grid-connected units to support the network voltage when faults occur in the transmission or distribution system. They consist of specific voltage curves that both synchronous generators and power electronic interfaced modules should satisfy. Although the initial motivation for the FRT design comes from faults in the transmission system, recent research in FRT emphasizes on faults in the distribution system and particularly at the PCC (after the transformer of the DERs) [20].

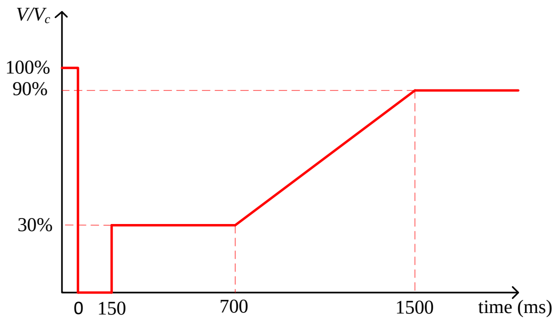

Figure 2. PCC voltage curve for the FRT operation of grid-connected units according to BDEW [3]

The curve of desired operation during faults according to BDEW can be seen in Fig. 2. When the PCC voltage is above 0.9 p.u., the DER should maintain its normal operation. Note that under more severe faults, a minimum time that the DER stays connected to the grid is introduced. For example, during a short circuit (PCC voltage becomes 0 p.u.), the DER should stay connected for at least 150 ms, while during a fault that leads to a PCC voltage of 0.7 p.u. for at least 700 ms.

Hence, during a significant voltage drop in the PCC voltage, the DER needs to increase the reactive power injection to the grid, in order to support the voltage, and also adjust the real power to avoid high currents. The desired reactive power to be injected often depends on the voltage drop ΔV of the PCC. For example, in [20], it is stated that the reactive current i_q, which affects the reactive power, is obtained as

$$i_q = K\,|\Delta V| \tag{7}$$

where K is the FRT gain. Based on this value, the active current, which affects the real power, is calculated according to the maximum apparent power requirement. FRT requirements differ from country to country at the moment since there is no generic guideline for the FRT operation, but in order for the electricity grids to become more resilient and the penetration level of DER to increase, it is believed that in the following years, a generic scheme will be proposed.

III. Proposed CLD controller with FRT capability

A. Controller design

The controller of a traditional grid-tied inverter with FRT capabilities should automatically change from the droop control (normal operation) to the FRT control, when a significant PCC voltage drop is identified. This introduces a change in both the real and the reactive power of the inverter.

In this paper, the CLD controller is extended to adopt an FRT capability by only changing the reactive power control during the fault. The real power will be automatically adjusted due to the inherent current-limiting property of the controller. In order to achieve this, the maximum capacity of the inverter should be utilized. To this end, the CLD controller with FRT capability takes the form

$$v = v_c + (1-w_q)(\sqrt{2}E^*\sin(\omega_g t+\delta) - wi), \tag{8}$$

with dynamics

$$\dot{w} = -c_w f(P,V_C)w_q^2 \tag{9}$$

$$\dot{w}_q = \frac{c_w(w-w_m)w_q}{\Delta w_m^2}f(P,V_c) - k_w\left(\frac{(w-w_m)^2}{\Delta w_m^2}+w_q^2-1\right)w_q \tag{10}$$

$$\dot{\delta} = c_\delta g(Q,\alpha,\omega_g)\delta_q^2 \tag{11}$$

$$\dot{\delta}_q = -\frac{c_\delta\delta\delta_q}{\Delta\delta_m^2}c_\delta g(Q,\alpha,\omega_g) - k_\delta\left(\frac{\delta^2}{\Delta\delta_m^2}+\delta_q^2-1\right)\delta_q, \tag{12}$$

where $f(P,V_c)$ and $g(Q,\alpha,\omega_g)$ are given by

$$f(P,V_c) = n(P_{set}-P)+K_e(E^*-V_c) \tag{13}$$

$$g(Q,\alpha,\omega_g) = \alpha(\omega^*-\omega_g) - m(\alpha Q_{set}+(1-\alpha)S_{max}-Q). \tag{14}$$

Note that although the dynamics of w and w_q are the same with the original CLD controller given in (3)-(4), the control input v and the dynamics of δ and δ_q are different for two main reasons: i) to fully utilize the capacity S_{max} of the inverter and ii) to inherit an FRT capability. A variable α has been introduced which takes values in the set $\{0,1\}$. It is clear that when $\alpha=1$, then the δ and δ_q dynamics of the original CLD controller become the same with (11)-(12), introducing the droop functions, while when $\alpha=0$, then the proposed controller achieves accurate reactive power regulation where the reference of the reactive power is S_{max} to maximize the reactive power injection to the grid. Based on the FRT requirements presented in Subsection II-B, the value of α should be 1 under normal conditions and change to 0 when the PCC voltage drops below 0.9pu. The proposed controller implementation is shown in Fig. 3 and the FRT algorithm is shown in Fig. 4.

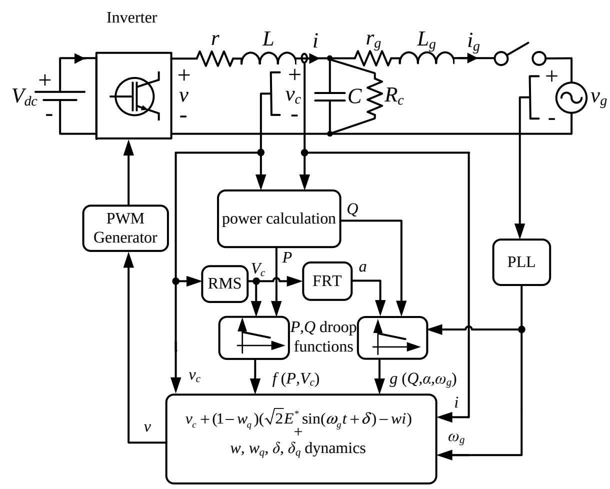

Figure 3. Implementation of the proposed CLD controller with FRT capability

B. Current-limiting property

Since the proposed controller changes only the reactive power injection during a fault, the current-limiting property should be guaranteed to maintain a limited apparent power. Hence the real power will be automatically adjusted.

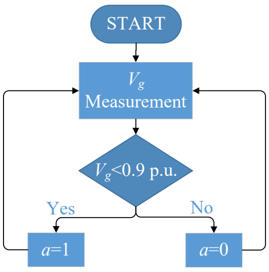

Figure 4. Proposed FRT algorithm

By applying the proposed controller (8) into the original system dynamics (1), the dynamics of the inverter current become

$$L\frac{di}{dt} = -(r+(1-w_q)w)i+(1-w_q)\sqrt{2}E^*\sin(\omega_g t+\delta). \quad (15)$$

Following the analysis of the original CLD dynamics for w and w_q, it holds true that $w \in [w_{min}, w_{max}] > 0$, where $w_{min} = w_m - \Delta w_m$, $w_{max} = w_m + \Delta w_m$, and $w_q \in [0,1]$ for all $t \geq 0$ (for details see [24]). Taking into account these properties, then, for system (15), consider the Lyapunov function candidate

$$V = \frac{1}{2}Li^2. \quad (16)$$

This actually represents the energy stored in the inductor L. The time derivative of V becomes after substituting (15) in the following

$$\begin{aligned}\dot{V} &= -(r+(1-w_q)w)i^2+(1-w_q)\sqrt{2}E^* i\sin(\omega_g t+\delta)\\ &\leq -(r+(1-w_q)w_{min})i^2+(1-w_q)\sqrt{2}E^*\left|i\right|\left|\sin(\omega_g t+\delta)\right|.\end{aligned}$$

This shows that $\dot{V} < 0$ when $|i| > \frac{(1-w_q)\sqrt{2}E^*|\sin(\omega_g t+\delta)|}{r+(1-w_q)w_{min}}$, proving that (15) is input-to-state stable (ISS) assuming as input the expression $(1-w_q)\sqrt{2}E^*\sin(\omega_g t+\delta)$. Since this expression is bounded, then the inverter current i is bounded for all $t \geq 0$. According to the ISS property, it holds true that

$$|i| \leq \frac{(1-w_q)\sqrt{2}E^*}{r+(1-w_q)w_{min}}, \forall t \geq 0,$$

if initially $i(0)$ satisfies the previous inequality. Since w_{min} is one of the controller parameters ($w_{min} = w_m - \Delta w_m$), by selecting

$$w_{min} = \frac{E^*}{I_{max}}, \quad (17)$$

where I_{max} is the maximum allowed RMS value of the inverter current, then

$$|i| \leq \frac{(1-w_q)}{r\frac{I_{max}}{E^*}+(1-w_q)}\sqrt{2}I_{max} \leq \sqrt{2}I_{max}, \quad (18)$$

since $(1-w_q) \geq 0$ and $r\frac{I_{max}}{E^*} > 0$. The previous inequality holds for any $t \geq 0$ and for any constant positive I_{max}. As a result

$$I \leq I_{max}, \forall t \geq 0, \quad (19)$$

where I is the RMS value of the inverter current, showing that the proposed controller introduces a current-limiting property below a given value I_{max}.

For the selection of the remaining controller parameters $w_{max} = w_m + \Delta w_m$, $\Delta\delta_m$, c_w, c_δ, k_w and k_δ, the reader is referred to [24]. It is worth noting that by selecting $\Delta\delta_m = 90^o$, the phase shift δ in the proposed controller (8) is bounded in the range $\delta \in [-90^o, 90^o]$ independently from the function $(\omega^* - \omega_g)\alpha + m(Q - \alpha Q_{set} - (1-\alpha)S_{max})$ inside (11)-(12). This practically corresponds to a limitation of the reactive power of the inverter between $[-S_{max}, S_{max}]$.

In order to understand how the current-limiting property results in a limit of the apparent power S, consider initially a normal and stiff grid with $V_g = E^*$ and by neglecting the small voltage drop between the PCC, i.e. capacitor voltage V_c, and the grid voltage V_g, it yields

$$S = V_c I \approx V_g I \leq E^* I_{max} = S_{max}. \quad (20)$$

Given the maximum apparent power of the inverter, then I_{max} can be selected as $I_{max} = \frac{S_{max}}{E^*}$.

However, when there is a grid fault and the grid voltage V_g drops by a percentage p, then according to (20), the proposed controller limits the apparent power below $(1-p)V_g I_{max}$. When the FRT is enabled, i.e. $p > 0.1$, then $\alpha = 0$ and according to (11), the dynamics of the phase shift δ become

$$\dot{\delta} = c_\delta m(Q - S_{max})\delta_q^2. \quad (21)$$

Note that S_{max} corresponds to the rated apparent power of the inverter, considering a normal grid. Since the apparent power S of the inverter is limited below $(1-p)V_g I_{max}$ due to the current-limiting property, then in (21) there is

$$\dot{\delta} = c_\delta m(Q - S_{max})\delta_q^2 \leq c_\delta m((1-p)V_g I_{max} - E^* I_{max})\delta_q^2 < 0.$$

This means that the phase shift δ will keep decreasing and since $\delta \in [-90^o, 90^o]$, due to the bounded control structure of (11)-(12) [24], then at the steady-state there is $\delta \to -90^o$. This means that $Q \to Q_e = (1-p)E^* I_{max} < S_{max}$, i.e. the reactive power will be regulated to the maximum apparent power under the grid voltage drop. Obviously, at the steady-state, the real power will automatically converge to zero since

$$P \to P_e = \sqrt{((1-p)E^* I_{max})^2 - Q_e^2} = 0.$$

This property indicates that the proposed controller requires only a change in the phase shift dynamics of δ which are related to the reactive power and the real power will be automatically reduced to zero to allow maximum reactive power injection with a current limitation to protect the inverter and at the same time support the grid voltage.

According to the BDEW guidelines, when the PCC voltage drops to 0.2 p.u., the DER unit should remain connected to the grid for 150 ms and inject as much reactive power as possible. When this time margin has passed, the fault is considered as permanent and the protection system should be triggered to trip the circuit breaker and disconnect the unit from the grid. Although the protection system is out of this paper's scope, the effect of the proposed controller to the protection system operation represents an interesting topic for future research.

IV. Simulation Results

In order to verify the desired operation of the proposed controller, a grid-connected single-phase inverter is simulated in Matlab/Simulink under normal and faulty grid conditions, since the implementation of the FRT algorithm in single-phase systems has shown an increasing interest recently [23], [22]. The power system and controller parameters are shown in Table I. Both the original CLD and the proposed CLD with FRT capability are investigated under the same scenario. The inverter is connected to the grid at 0.1 s. Initially, P is set to 150 W, and Q is set to 0 Var, while at 0.6 s, the real power changes to 300 W and the reactive power increases to 200 Var. As it is shown in Fig. 5, both the original and the proposed CLD lead the real and the reactive power of the inverter to the desired values. The P-droop and the Q-droop functions are enabled at 1 s, and it is clear that both the real and the reactive power drop since the output voltage V_c is above the rated value and the grid frequency ω_g is slightly below the rated frequency ω^*, respectively. Until this point, the responses of the original and the proposed CLD with FRT are identical, proving that the proposed version maintains the original CLD behaviour under a normal grid.

Table I
System and Controller Parameters

Parameters	Values	Parameters	Values
L, L_g	2.2 mH	ω^*	2π x 50 rad/s
r, r_g	0.5 Ω	ω_g	2π x 49.98 rad/s
C	10 μF	I_{max}	8 A
$V_g = E^*$	110 V	w_m	318.25 Ω
S_n	880 VA	Δw_m	304.5 Ω
c_w	348	K_e	10
c_δ	15.7	k_w, k_δ	1000
n	0.0625	m	0.0036

To investigate the controller performance under a faulty grid, at 2s, a voltage sag occurs and the grid voltage drops by 30% and the fault is self-cleared at 2.3s. As shown in Fig. 5a, when the CLD with the FRT is adopted, the active power reduces during the fault, opposed to the original CLD. This is caused by the fact that the proposed controller maximizes the reactive power injection, as shown in Fig. 5b. In this case, due to the current-limiting property of the proposed controller and the fact that reactive power is being increased in order to reach S_{max} (Fig. 5d), the real power automatically drops to zero. The support to the PCC voltage is clear in Fig. 5c, where it is observed that the RMS output voltage of the proposed CLD with the FRT is higher than the one with the original CLD. It is also observed from the RMS current response in Fig. 5d that during the fault, the current with the CLD equipped with the FRT reaches the maximum value, while the original CLD limits the currents to a lower value that corresponds to the percentage of the voltage dip. This clearly indicates the ability of the proposed controller to fully utilize the entire capacity of the inverter. Finally, the time response of the controller states w and δ are given in Fig. 6a and Fig. 6b, respectively. Since the dynamics of w are the same in both controllers, it is obvious that the response of w is identical in both scenarios. However, the phase shifting δ differs since in the case of the proposed

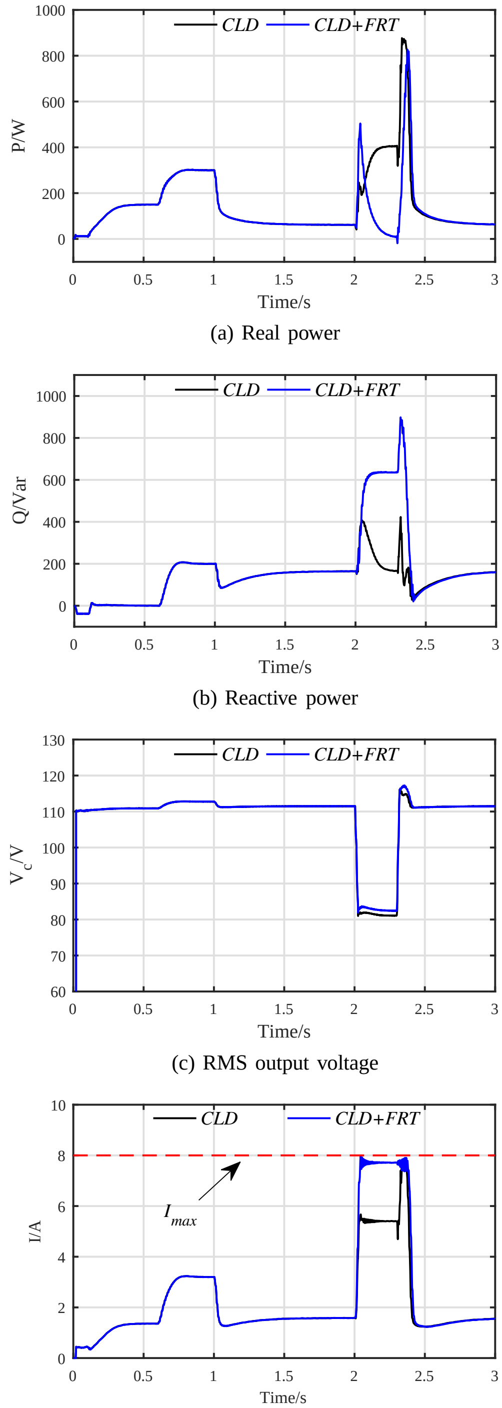

(a) Real power

(b) Reactive power

(c) RMS output voltage

(d) RMS inverter current

Figure 5. Simulation results of the grid-connected inverter using the proposed CLD equipped with the FRT algorithm compared to the original CLD

CLD with the FRT, it tends to -90^o during the fault in order to maximize the injection of the reactive power.

V. Conclusions

A nonlinear droop controller with current-limiting capability that additionally complies with the fault-ride-through requirements, as proposed by international boards and organizations, has been developed. During a sudden grid voltage dip, it is

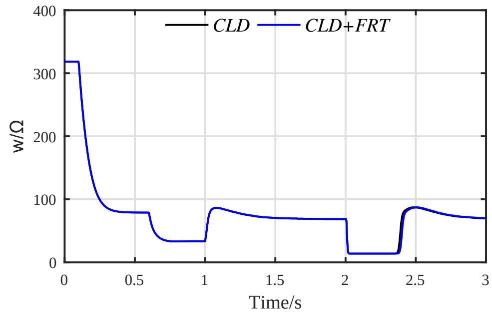

(a) Controller state w

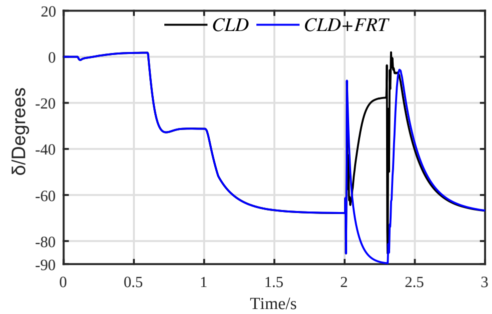

(b) Controller state δ

Figure 6. Time response of the controller states w and δ using the proposed CLD equipped with the FRT algorithm and the original CLD

proven that the proposed controller maximizes the reactive power injection to the grid in order to support the grid voltage, while inherently protecting the inverter from large currents. Due to this current-limiting property, the FRT algorithm is simplified, since the injected real power automatically drops. It is shown that the proposed controller can fully utilize the capacity of the grid-connected unit. Extensive simulation results have verified the proposed control approach.

References

[1] Math H. Bollen and Fainan Hassan. *Integration of Distributed Generation in the Power System*. Wiley, 2011.

[2] N. Bottrell and T. C. Green. Comparison of current-limiting strategies during fault ride-through of inverters to prevent latch-up and wind-up. *IEEE Trans. Power Electron.*, 29(7):3786–3797, 2014.

[3] Bundesverband der Energie und Wasserwirtschaft (BDEW). Technical guideline: Generating plants connected to the medium-voltage network, 2008.

[4] A. Camacho, M. Castilla, J. Miret, A. Borrell, and L. G. de Vicuna. Active and reactive power strategies with peak current limitation for distributed generation inverters during unbalanced grid faults. *IEEE Transactions on Industrial Electronics*, 62(3):1515–1525, March 2015.

[5] A. Camacho, M. Castilla, J. Miret, R. Guzman, and A. Borrell. Reactive power control for distributed generation power plants to comply with voltage limits during grid faults. *IEEE Transactions on Power Electronics*, 29(11):6224–6234, Nov 2014.

[6] M.C. Chandorkar, D.M. Divan, and R. Adapa. Control of parallel connected inverters in standalone ac supply systems. *IEEE Transactions on Industry Applications*, 29(1):136–143, Jan. 1993.

[7] H. C. Chen, C. T. Lee, P. T. Cheng, R. Teodorescu, and F. Blaabjerg. A low-voltage ride-through technique for grid-connected converters with reduced power transistors stress. *IEEE Transactions on Power Electronics*, 31(12):8562–8571, Dec 2016.

[8] W. F. d. Souza, M. A. Severo-Mendes, and L. A. C. Lopes. Power sharing control strategies for a three-phase microgrid in different operating condition with droop control and damping factor investigation. *IET Renewable Power Generation*, 9(7):831–839, 2015.

[9] ENTSO-E. Nework code for requirements for grid connection - applicable to all generators, 2013.

[10] J. M. Guerrero, Luis Garcia de Vicuna, J. Matas, M. Castilla, and J. Miret. Output impedance design of parallel-connected ups inverters with wireless load-sharing control. *IEEE Transactions on Industrial Electronics*, 52(4):1126–1135, Aug 2005.

[11] J. M. Guerrero, J. Matas, L. Garcia de Vicuna, M. Castilla, and J. Miret. Decentralized control for parallel operation of distributed generation inverters using resistive output impedance. *IEEE Transactions on Industrial Electronics*, 54(2):994–1004, April 2007.

[12] Y. W. Li and C. N. Kao. An accurate power control strategy for power-electronics-interfaced distributed generation units operating in a low-voltage multibus microgrid. *IEEE Transactions on Power Electronics*, 24(12):2977–2988, Dec 2009.

[13] Antonios Marinopoulos, Fabio Papandrea, Muhamad Reza, Staffan Norrga, Filippo Spertino, and Roberto Napoli. Grid integration aspects of large solar pv installations: Lvrt capability and reactive power/voltage support requirements. In *2011 IEEE Trondheim PowerTech*, 2011.

[14] National Grid. Fault ride through, 2009.

[15] National Grid Electricity Transmission plc. The grid code, 2016.

[16] D. E. Olivares, A. Mehrizi-Sani, A. H. Etemadi, C. A. Canizares, R. Iravani, M. Kazerani, A. H. Hajimiragha, O. Gomis-Bellmunt, M. Saeedifard, R. Palma-Behnke, G. A. Jimenez-Estevez, and N. D. Hatziargyriou. Trends in microgrid control. *IEEE Transactions on Smart Grid*, 5(4):1905–1919, July 2014.

[17] A. D. Paquette and D. M. Divan. Virtual impedance current limiting for inverters in microgrids with synchronous generators. *IEEE Trans. Ind. Appl.*, 51(2):1630–1638, 2015.

[18] A. D. Paquette and D. M. Divan. Virtual impedance current limiting for inverters in microgrids with synchronous generators. *IEEE Transactions on Industry Applications*, 51(2):1630–1638, March 2015.

[19] P. Piagi and R. H. Lasseter. Autonomous control of microgrids. In *2006 IEEE Power Engineering Society General Meeting*, pages 1–8, 2006.

[20] Ioannis-Thomas Theologitis, Eckehard Troester, and Thomas Ackermann. Aspects of a generic photovoltaic model examined under the gemran grid code for medium voltage. In *1st International Workshop on Integration of Solar Power*, 2011.

[21] B. Weise. Impact of k-factor and active current reduction during fault-ride-through of generating units connected via voltage-sourced converters on power system stability. *IET Renewable Power Generation*, 9(1):25–36, 2015.

[22] Y. Yang, F. Blaabjerg, and H. Wang. Low-voltage ride-through of single-phase transformerless photovoltaic inverters. *IEEE Transactions on Industry Applications*, 50(3):1942–1952, May 2014.

[23] Y. Yang, F. Blaabjerg, and Z. Zou. Benchmarking of grid fault modes in single-phase grid-connected photovoltaic systems. *IEEE Transactions on Industry Applications*, 49(5):2167–2176, Sept 2013.

[24] Q. C. Zhong and G. C. Konstantopoulos. Current-limiting droop control of grid-connected inverters. *IEEE Transactions on Industrial Electronics*, 64(7):5963–5973, July 2017.

[25] Q. C. Zhong and Y. Zeng. Universal droop control of inverters with different types of output impedance. *IEEE Access*, 4:702–712, 2016.